Weierstraß-Institut
für Angewandte Analysis und Stochastik

im Forschungsverbund Berlin e.V.

Preprint ISSN 0946 – 8633

A direct simulation Monte Carlo method for the Uehling-Uhlenbeck-Boltzmann equation

Alejandro L. Garcia[1], Wolfgang Wagner[2]

submitted: 20th August 2002

[1] Institute for Scientific Computing Research
Lawrence Livermore National Laboratory
Livermore, California 94550, USA
Permanent address: Physics Department
San Jose State University
San Jose, California 95192, USA
E-Mail: algarcia@algarcia.org

[2] Weierstrass Institute for
Applied Analysis and Stochastics
Mohrenstrasse 39
D-10117 Berlin, Germany
E-Mail: wagner@wias-berlin.de

No. 763
Berlin 2002

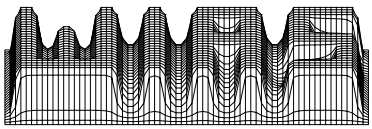

1991 *Mathematics Subject Classification.* 65C05, 76P05, 82C40.

Key words and phrases. Uehling-Uhlenbeck-Boltzmann equation, Fermi-Dirac case, Bose-Einstein case, DSMC algorithm, numerical experiments.

Edited by
Weierstraß-Institut für Angewandte Analysis und Stochastik (WIAS)
Mohrenstraße 39
D — 10117 Berlin
Germany

Fax: + 49 30 2044975
E-Mail: preprint@wias-berlin.de
World Wide Web: http://www.wias-berlin.de/

Abstract

In this paper we describe a DSMC algorithm for the Uehling-Uhlenbeck-Boltzmann equation in terms of Markov processes. This provides a unifying framework for both the classical Boltzmann case as well as the Fermi-Dirac and Bose-Einstein cases. We establish the foundation of the algorithm by demonstrating its link to the kinetic equation. By numerical experiments we study its sensitivity to the number of simulation particles and to the discretization of the velocity space, when approximating the steady state distribution.

Contents

1. Introduction

The recent landmark experiments of Bose-Einstein condensation have generated significant interest in quantum ideal gases (see [8] and references therein). Kinetic theory is useful in the study of a quantum gas, especially when the particle dynamics can be decomposed into two-body collisions and a mean field potential. For this regime, Uehling and Uhlenbeck [16] extended the Boltzmann equation to quantum systems by including the Pauli factor. In the spatially homogeneous case, this equation takes the form

$$\frac{\partial}{\partial t} f(t,v) = \int_{\mathcal{R}^3} dw \int_{\mathcal{S}^2} de\, B(v,w,e) \Big[(1+\theta f(t,v))\,(1+\theta f(t,w))\, f(t,v^*)\, f(t,w^*) - (1+\theta f(t,v^*))\,(1+\theta f(t,w^*))\, f(t,v)\, f(t,w) \Big], \tag{1.1}$$

with initial condition $f(0,v) = f_0(v)$.

The postcollision velocities corresponding to $v, w \in \mathcal{R}^3$ are

$$v^*(v,w,e) = v + e\,(e, w-v)\,, \quad w^*(v,w,e) = w - e\,(e, w-v)\,, \qquad e \in \mathcal{S}^2\,, \tag{1.2}$$

where $\mathcal{S}^2 \subset \mathcal{R}^3$ is the unit sphere, and $(.,.)$ denotes the scalar product in the Euclidean space $\mathcal{R}^3$. The function B is the collision kernel, which, in case of hard sphere molecules, takes the form $B(v,w,e) = \text{const}\,|(e, w-v)|$. Note that $n = \int_{\mathcal{R}^3} f_0(v)\, dv$ is the average number of physical particles per unit volume in position space. Equation (1.1) includes (namely for $\theta = 0$) the **Boltzmann** equation of classical statistics as a special case. It differs from the latter in the case of **Bose-Einstein** statistics ($\theta = +1$) and in the case of **Fermi-Dirac** statistics ($\theta = -1$). The case $\theta = +1$ has been studied recently in [14].

Direct simulation Monte Carlo (DSMC) has been the most widely used numerical algorithm for the classical Boltzmann equation [4]. Stochastic particle algorithms for the Uehling-Uhlenbeck-Boltzmann (UUB) equation were first developed to simulate the Fermi-Dirac dynamics of nucleons during heavy ion collisions [3], [2], [5]. These numerical methods were later reformulated into a DSMC-based framework by Lang, et al. [12]. Similar Monte Carlo algorithms have been used to study the dynamics of cooling [17] and trapping [6] in Bose-Einstein condensation. Dense gas corrections to the UUB equation have been modelled using the Consistent Boltzmann Algorithm [1], a dense gas variant of DSMC. This algorithm has been used to include virial corrections to UUB simulations [11], [15]. Its asymptotic properties in the Boltzmann case have been studied in [9].

In this paper we describe a DSMC algorithm for the Uehling-Uhlenbeck-Boltzmann equation in terms of Markov processes. This provides a unifying framework for both the classical Boltzmann case as well as the Fermi-Dirac and Bose-Einstein cases. We establish the foundation of the algorithm by demonstrating its link to equation (1.1). Using numerical experiments we study its sensitivity to the number of simulation particles and to the discretization of the velocity space, when approximating the steady state distribution.

The paper is organized as follows. In Section 2 we give a detailed description of the DSMC algorithm starting from a corresponding Markov jump process. Section 3 provides a heuristic derivation of the limiting equation when the number of simulation particles tends to infinity. In Section 4 we study the equilibrium behaviour of the solution to the

UUB equation. Finally, Section 5 contains results of numerical experiments. We calculate approximations to the equilibrium solution using the particle algorithm. We study the error depending on the numerical parameters like particle number or number of cells in the velocity space.

2. Description of the algorithm

We introduce a Markov process

$$Z(t) = \Big(V_1(t), \dots, V_N(t)\Big), \qquad t \geq 0\,, \tag{2.1}$$

defined by the infinitesimal generator

$$\mathcal{A}(\Phi)(z) = \frac{n}{2N} \sum_{1 \leq i \neq j \leq N} \int_{\mathcal{S}^2} Q(z,i,j,e) \Big[\Phi(J(z,i,j,e)) - \Phi(z)\Big]\, de\,, \tag{2.2}$$

where

$$z = (v_1, \dots, v_N) \in \big(\mathcal{R}^3\big)^N = \mathcal{Z} \tag{2.3}$$

and N is the number of simulation particles. The jump transformation is (cf. (1.2))

$$[J(z,i,j,e)]_k = \begin{cases} v_k & , \text{ if } \quad k \neq i,j\,, \\ v^*(v_i, v_j, e)\,, & \text{ if } \quad k = i\,, \\ w^*(v_i, v_j, e)\,, & \text{ if } \quad k = j\,. \end{cases} \tag{2.4}$$

The intensity function has the form

$$Q(z,i,j,e) = Y\left(\frac{n}{N}\sum_{k=1}^{N} g(v^*(v_i,v_j,e), v_k), \frac{n}{N}\sum_{k=1}^{N} g(w^*(v_i,v_j,e), v_k)\right) B(v_i, v_j, e)\,, \tag{2.5}$$

where g is some mollifying kernel,

$$g(v,w) = g(w,v) \geq 0\,, \qquad \int_{\mathcal{R}^3} g(v,w)\, dw = 1\,, \tag{2.6}$$

intended for approximating Dirac's delta-function. The concrete form of g as well as of the non-negative function Y will be specified later.

For numerical purposes, we rewrite the generator (2.2) in the form

$$\mathcal{A}(\Phi)(z) = \int_{\mathcal{Z}} \Big[\Phi(\bar{z}) - \Phi(z)\Big]\, \hat{\mathcal{Q}}(z, d\bar{z})\,,$$

where

$$\hat{\mathcal{Q}}(z, d\bar{z}) = \tag{2.7}$$
$$\frac{n}{2N} \sum_{1 \leq i \neq j \leq N} \int_{\mathcal{S}^2} \Big\{\delta_{J(z,i,j,e)}(d\bar{z})\, Q(z,i,j,e) + \delta_z(d\bar{z}) \Big[\hat{Y}(z)\, \hat{B}(z) - Q(z,i,j,e)\Big]\Big\}\, de$$

and δ denotes the Dirac measure. The functions $\hat{B}$ and $\hat{Y}$ are such that (cf. (2.5))

$$Y\left(\frac{n}{N}\sum_{k=1}^{N} g(v^*(v_i,v_j,e),v_k), \frac{n}{N}\sum_{k=1}^{N} g(w^*(v_i,v_j,e),v_k)\right) \le \hat{Y}(z)\,, \qquad \forall\ z\in\mathcal{Z}\,, \quad (2.8)$$

and

$$B(v_i,v_j,e) \le \hat{B}(z)\,, \qquad \forall\ 1\le i\ne j\le N\,, \quad e\in\mathcal{S}^2\,, \quad z\in\mathcal{Z}\,. \quad (2.9)$$

Thus, the pathwise behaviour of the process is as follows. Coming to a state (2.3), the process stays there for a **random waiting time**, which has an exponential distribution with the parameter (cf. (2.7))

$$\hat{\pi}(z) = \hat{\mathcal{Q}}(z,\mathcal{Z}) = 2\pi\, n\, \hat{Y}(z)\, \hat{B}(z)\, (N-1)\,. \quad (2.10)$$

Then the process jumps into a state $\bar{z}$, which is distributed according to the jump distribution

$$\hat{\pi}(z)^{-1}\, \hat{\mathcal{Q}}(z,d\bar{z}) =$$
$$\frac{1}{N\,(N-1)} \sum_{1\le i\ne j\le N} \frac{1}{4\pi}\int_{\mathcal{S}^2} \left\{ \delta_{J(z,i,j,e)}(d\bar{z})\, \frac{Q(z,i,j,e)}{\hat{Y}(z)\,\hat{B}(z)} + \delta_z(d\bar{z}) \left[1 - \frac{Q(z,i,j,e)}{\hat{Y}(z)\,\hat{B}(z)}\right]\right\}.$$

Consequently, first the parameters $i\,, j$ and e are generated **uniformly**. Given $i\,, j$ and $e\,,$ the jump is **fictitious**, i.e. the new state is $\bar{z} = z\,,$ with probability

$$1 - \frac{Q(z,i,j,e)}{\hat{Y}(z)\,\hat{B}(z)}\,. \quad (2.11)$$

Otherwise, the new state is $\bar{z} = J(z,i,j,e)\,.$

For calculating the quantity (2.11), one needs to evaluate the **empirical density** (cf. (2.5))

$$\hat{f}(z,v) \;\; = \;\; \frac{n}{N}\sum_{k=1}^{N} g(v,v_k)\,, \quad (2.12)$$

for $v = v^*(v_i,v_j,e)$ and $v = w^*(v_i,v_j,e)\,.$ Note that (2.6) implies

$$\int_{\mathcal{R}^3} \hat{f}(z,v)\, dv = n\,, \qquad \forall z\in\mathcal{Z}\,.$$

For numerical purposes, it is convenient to introduce some partition $\mathcal{V}_l\,,\ l = 1,...,M\,,$ of the velocity space and to use the function

$$g(v,w) = \sum_{l=1}^{M} \frac{1}{|\mathcal{V}_l|}\, \chi_{\mathcal{V}_l}(v)\, \chi_{\mathcal{V}_l}(w)\,, \quad (2.13)$$

where χ denotes the indicator function. Let $N_l\,,\ l = 1,...,M\,,$ be the number of particles with velocities in cell $\mathcal{V}_l\,.$ Then the empirical density (2.12) takes the form

$$\hat{f}(z,v) = \frac{n\, N_{l(v)}}{N\,|\mathcal{V}_{l(v)}|}\,, \qquad v\in\mathcal{R}^3\,, \quad (2.14)$$

where $l(v)$ denotes the number of the cell to which v belongs. Note that the function (2.14) is constant in each cell.

The following algorithm is obtained.

0. Generate the initial state z so that (2.12) approximates f_0 for large N.

1. Given z calculate the time step

$$\frac{1}{2\pi\, n\, \hat{Y}(z)\, \hat{B}(z)\, (N-1)}$$

according to (2.10).

2. Generate i, j, e uniformly and calculate

$$v_i^* = v^*(v_i, v_j, e)\,, \qquad v_j^* = w^*(v_i, v_j, e)$$

according to (2.4).

3. With probability (2.11), i.e. if

$$\frac{Y(\hat{f}(z, v_i^*), \hat{f}(z, v_j^*))}{\hat{Y}(z)}\, \frac{B(v_i, v_j, e)}{\hat{B}(z)} \;\leq\; \mathrm{RAND}\,,$$

go to **1.**

4. Replace $v_i\,, v_j$ by $v_i^*\,, v_j^*$.

5. Update $\hat{B}$, $\hat{f}$, $\hat{Y}$ and go to **1.**

Some remarks: First, in the Boltzmann case $Y \equiv 1$, the procedure differs slightly from standard DSMC. This is due to the fact that in general Y depends on e so that this parameter also must be generated **before** the rejection. Second, note that the function $\hat{Y}$ in (2.8) can be adapted during the process of computation, similar to the adaption of the function $\hat{B}$ in (2.9) depending on the maximum relative velocity. Third, even if $M = \infty$, the sum (2.13) remains finite. Alternatively, one considers the set outside some (big) ball in the velocity space as the last cell. The empirical density is there approximated by zero. Finally, the limiting equation (as $N \to \infty$) for this Markov process is the UUB equation (1.1), for the choice

$$Y(x, y) = (1 + \theta\, x)\, (1 + \theta\, y)\,, \qquad x, y \in \mathcal{R}\,. \tag{2.15}$$

The derivation of this result is presented in the next section.

3. Derivation of the limiting equation

The Markov process (2.1) satisfies

$$\Phi(Z(t)) = \Phi(Z(0)) + \int_0^t \mathcal{A}(\Phi)(Z(s))\, ds + M(t)\,, \qquad t \geq 0\,, \tag{3.1}$$

where $M(t)$ is some martingale term. We consider (cf. (2.3))

$$\Phi(z) = \frac{n}{N} \sum_{i=1}^{N} \varphi(v_i)\,, \qquad z \in \mathcal{Z}\,,$$

for appropriate test functions φ. Note that

$$\Phi(Z(t)) = \frac{n}{N} \sum_{i=1}^{N} \varphi(V_i(t)) \quad =: \quad \int_{\mathcal{R}^3} \varphi(v)\, \nu^{(N)}(t, dv)\,, \tag{3.2}$$

where $\nu^{(N)}$ is the empirical measure of the particle system (2.1). According to (2.2)–(2.5), one obtains

$$\begin{aligned}
&\mathcal{A}(\Phi)(z) = \\
&\quad \frac{n^2}{2N^2} \sum_{1 \le i \ne j \le N} \int_{\mathcal{S}^2} Y\left(\frac{n}{N} \sum_{k=1}^{N} g(v^*(v_i, v_j, e), v_k), \frac{n}{N} \sum_{k=1}^{N} g(w^*(v_i, v_j, e), v_k) \right) \times \\
&\quad B(v_i, v_j, e) \Big[\varphi(v^*(v_i, v_j, e)) + \varphi(w^*(v_i, v_j, e)) - \varphi(v_i) - \varphi(v_j) \Big] de
\end{aligned}$$

and

$$\begin{aligned}
&\mathcal{A}(\Phi)(Z(s)) = \\
&\quad \frac{1}{2} \int_{\mathcal{R}^3} \int_{\mathcal{R}^3} \int_{\mathcal{S}^2} Y\left(\int_{\mathcal{R}^3} g(v^*, u)\, \nu^{(N)}(s, du), \int_{\mathcal{R}^3} g(w^*, u)\, \nu^{(N)}(s, du) \right) \times \\
&\quad B(v, w, e) \Big[\varphi(v^*) + \varphi(w^*) - \varphi(v) - \varphi(w) \Big] de\, \nu^{(N)}(s, dv)\, \nu^{(N)}(s, dw) + O(N^{-1})\,,
\end{aligned} \tag{3.3}$$

where the functions v^*, w^* depend on the arguments v, w, e as defined in (1.2).

Suppose that the following relations are fulfilled as $N \to \infty$,

$$\nu^{(N)}(t) \to F(t)\,, \qquad M^{(N)}(t) \to 0\,, \qquad \forall t \ge 0\,,$$

for some deterministic measure-valued function $F(t)$. Under certain assumptions concerning this convergence, one can conclude from (3.1), (3.3) that the limit $F(t)$ satisfies the equation

$$\begin{aligned}
&\int_{\mathcal{R}^3} \varphi(v)\, F(t, dv) = \int_{\mathcal{R}^3} \varphi(v)\, F_0(dv) \\
&\quad + \quad \frac{1}{2} \int_0^t \int_{\mathcal{R}^3} \int_{\mathcal{R}^3} \int_{\mathcal{S}^2} Y\left(\int_{\mathcal{R}^3} g(v^*, u)\, F(s, du), \int_{\mathcal{R}^3} g(w^*, u)\, F(s, du) \right) \times \\
&\qquad B(v, w, e) \Big[\varphi(v^*) + \varphi(w^*) - \varphi(v) - \varphi(w) \Big] de\, F(s, dv)\, F(s, dw)\, ds\,.
\end{aligned}$$

The differential form with respect to t is

$$\begin{aligned}
&\frac{d}{dt} \int_{\mathcal{R}^3} \varphi(v)\, F(t, dv) = \frac{1}{2} \int_{\mathcal{R}^3} \int_{\mathcal{R}^3} \int_{\mathcal{S}^2} \beta(t, v^*, w^*) \times \\
&\qquad B(v, w, e) \Big[\varphi(v^*) + \varphi(w^*) - \varphi(v) - \varphi(w) \Big] de\, F(t, dv)\, F(t, dw)\,,
\end{aligned} \tag{3.4}$$

with the initial condition

$$F_0 = \lim_{N\to\infty} \nu^{(N)}(0)\,, \tag{3.5}$$

where we denote

$$\beta(t,x,y) = Y\left(\int_{\mathcal{R}^3} g(x,u)\,F(t,du), \int_{\mathcal{R}^3} g(y,u)\,F(t,du)\right). \tag{3.6}$$

Note that, in case (2.13),

$$\int_{\mathcal{R}^3} g(v,u)\,F(t,du) = \frac{1}{|\mathcal{V}_{l(v)}|}\,F(t,\mathcal{V}_{l(v)})\,, \qquad \forall v\in\mathcal{R}^3\,,$$

and that (3.5) implies (cf. (3.2))

$$F_0(\mathcal{R}^3) = \lim_{N\to\infty} \nu^{(N)}(0,\mathcal{R}^3) = n\,.$$

Note that the conservation properties are derived from (3.4), as in the Boltzmann case $Y\equiv 1$, for $\varphi = 1, v, \|v\|^2$.

Assume the limiting measures have densities,

$$F(t,dv) = f(t,v)\,dv\,,$$

the function Y is symmetric, and

$$B(v,w,e) = B(v^*,w^*,e) = B(w,v,e) = B(v,w,-e)\,. \tag{3.7}$$

Note that the hard sphere kernel satisfies (3.7). Applying the substitution $(v^*,w^*)\to(v,w)$, the terms at the right-hand side of equation (3.4) transform according to

$$\int_{\mathcal{R}^3}\int_{\mathcal{R}^3}\int_{\mathcal{S}^2} \beta(t,v^*,w^*)\,B(v,w,e)\,\varphi(v^*)\,f(t,v)\,f(t,w)\,de\,dv\,dw =$$
$$\int_{\mathcal{R}^3}\int_{\mathcal{R}^3}\int_{\mathcal{S}^2} \beta(t,v,w)\,B(v,w,e)\,\varphi(v)\,f(t,v^*)\,f(t,w^*)\,de\,dv\,dw\,.$$

Removing the test functions, one obtains

$$\frac{\partial}{\partial t}\,f(t,v) = \tag{3.8}$$
$$\int_{\mathcal{R}^3} dw \int_{\mathcal{S}^2} de\,B(v,w,e)\Big[\beta(t,v,w)\,f(t,,v^*)\,f(t,w^*) - \beta(t,v^*,w^*)\,f(t,v)\,f(t,w)\Big].$$

If

$$g(x,y) = g^{(N)}(x,y) \;\;\to\;\; \delta(x-y) \qquad \text{as} \quad N\to\infty\,,$$

then (cf. (3.6)) $\beta(t,x,y) = Y(f(t,x),f(t,y))$, and equation (3.8) takes the form

$$\frac{\partial}{\partial t}\,f(t,v) = \int_{\mathcal{R}^3} dw \int_{\mathcal{S}^2} de\,B(v,w,e)\times \tag{3.9}$$
$$\Big[Y(f(t,v),f(t,w))\,f(t,v^*)\,f(t,w^*) - Y(f(t,v^*),f(t,w^*))\,f(t,v)\,f(t,w)\Big].$$

Equation (1.1) is obtained from (3.9) for the choice (2.15), with the particular cases $\theta = 1$ (Bose-Einstein), $\theta = 0$ (Boltzmann) and $\theta = -1$ (Fermi-Dirac). Note that since the function Y should be non-negative, it is more accurate to define (2.15) for $\theta < 0$ as

$$Y(x,y) = (1+\theta\,x)^+(1+\theta\,y)^+,$$

where $a^+ = a$ if $a > 0$ and $a^+ = 0$ otherwise.

4. Equilibrium behavior

First we recall the derivation of an **H-theorem** (cf., e.g., [13, Section 5.4.3]). Let f be a solution to equation (3.9) with Y as in (2.15). Defining

$$H(t) = \int_{\mathcal{R}^3} \left[f(t,v)\, \log f(t,v) - \frac{1}{\theta}\,(1+\theta\, f(t,v)) \log(1+\theta\, f(t,v)) \right] dv$$

one obtains

$$\begin{aligned} &\frac{d}{dt}\, H(t) = \\ &\qquad \int_{\mathcal{R}^3} \left[\frac{\partial}{\partial t}\, f(t,v)\, \log f(t,v) + \frac{\partial}{\partial t}\, f(t,v) - \frac{\partial}{\partial t}\, f(t,v)\, \log(1+\theta\, f(t,v)) - \frac{\partial}{\partial t}\, f(t,v) \right] dv \\ &= \int_{\mathcal{R}^3} \left[\frac{\partial}{\partial t}\, f(t,v)\, \log \frac{f(t,v)}{1+\theta\, f(t,v)} \right] dv\,. \end{aligned} \tag{4.1}$$

Note that the case $\theta = 0$ is easily covered, but in the case $\theta < 0$ the condition

$$f(t,v) \;<\; -\frac{1}{\theta} \tag{4.2}$$

has to be assumed. Using (3.9) and the notation $s(t,v) = 1 + \theta\, f(t,v)$, the right-hand side of (4.1) takes the form

$$\begin{aligned} &\int_{\mathcal{R}^3} dv \int_{\mathcal{R}^3} dw \int_{\mathcal{S}^2} de\, B(v,w,e) \times \\ &\qquad \Big[s(t,v)\, s(t,w)\, f(t,v^*)\, f(t,w^*) - s(t,v^*)\, s(t,w^*)\, f(t,v)\, f(t,w) \Big] \log \frac{f(t,v)}{s(t,v)} \\ &= \int_{\mathcal{R}^3} dv \int_{\mathcal{R}^3} dw \int_{\mathcal{S}^2} de\, B(v,w,e) \times \\ &\qquad \Big[s(t,v)\, s(t,w)\, f(t,v^*)\, f(t,w^*) - s(t,v^*)\, s(t,w^*)\, f(t,v)\, f(t,w) \Big] \log \frac{f(t,w)}{s(t,w)} \\ &= -\int_{\mathcal{R}^3} dv \int_{\mathcal{R}^3} dw \int_{\mathcal{S}^2} de\, B(v,w,e) \times \\ &\qquad \Big[s(t,v)\, s(t,w)\, f(t,v^*)\, f(t,w^*) - s(t,v^*)\, s(t,w^*)\, f(t,v)\, f(t,w) \Big] \log \frac{f(t,v^*)}{s(t,v^*)} \\ &= -\int_{\mathcal{R}^3} dv \int_{\mathcal{R}^3} dw \int_{\mathcal{S}^2} de\, B(v,w,e) \times \\ &\qquad \Big[s(t,v)\, s(t,w)\, f(t,v^*)\, f(t,w^*) - s(t,v^*)\, s(t,w^*)\, f(t,v)\, f(t,w) \Big] \log \frac{f(t,w^*)}{s(t,w^*)} \\ &= \frac{1}{4} \int_{\mathcal{R}^3} dv \int_{\mathcal{R}^3} dw \int_{\mathcal{S}^2} de\, B(v,w,e) \times \\ &\qquad \Big[s(t,v)\, s(t,w)\, f(t,v^*)\, f(t,w^*) - s(t,v^*)\, s(t,w^*)\, f(t,v)\, f(t,w) \Big] \times \\ &\qquad \log \frac{f(t,v)\, f(t,w)\, s(t,v^*)\, s(t,w^*)}{s(t,v)\, s(t,w)\, f(t,v^*)\, f(t,w^*)}\,. \end{aligned} \tag{4.3}$$

From $(b-a)\log\frac{a}{b} \le 0$ and (4.1), (4.3) one obtains

$$\frac{d}{dt}H(t) \le 0\,.$$

Next we consider the problem of the **steady state** p (cf. [7, Ch. 17.5]). From (3.9) one obtains

$$\frac{p(v^*)\,p(w^*)}{Y(p(v^*),p(w^*))} = \frac{p(v)\,p(w)}{Y(p(v),p(w))} \tag{4.4}$$

as a sufficient condition. Assuming

$$Y(x,y) = \tilde{Y}(x)\,\tilde{Y}(y)\,, \tag{4.5}$$

condition (4.4) takes the form

$$\log\frac{p(v^*)}{\tilde{Y}(p(v^*))} + \log\frac{p(w^*)}{\tilde{Y}(p(w^*))} = \log\frac{p(v)}{\tilde{Y}(p(v))} + \log\frac{p(w)}{\tilde{Y}(p(w))}\,. \tag{4.6}$$

Since $\psi(v^*)+\psi(w^*) = \psi(v)+\psi(w)$ implies $\psi(v) = c_1 + c_2\,\|v-\bar{v}\|^2$, for some $c_1, c_2 \in \mathcal{R}$ and $\bar{v} \in \mathcal{R}^3$, we obtain from (4.6)

$$p(v) = \tilde{Y}(p(v))\,\exp\left(c_1 + c_2\,\|v-\bar{v}\|^2\right). \tag{4.7}$$

The function (2.15) satisfies (4.5), with $\tilde{Y}(x) = 1+\theta\,x$. Thus, (4.7) implies

$$p(v) = \frac{\exp(c_1+c_2\,\|v-\bar{v}\|^2)}{1-\theta\,\exp(c_1+c_2\,\|v-\bar{v}\|^2)} = \frac{1}{\exp(-c_1-c_2\,\|v-\bar{v}\|^2)-\theta}\,. \tag{4.8}$$

The parameters c_1, c_2 and $\bar{v}$ have to be chosen to fit the conserved quantities. Necessary conditions (for positivity and integrability) are

$$\exp(-c_1) > \theta\,, \qquad c_2 < 0\,. \tag{4.9}$$

Note that, in the case $\theta < 0$, condition $p(v) < -\frac{1}{\theta}$ (cf. (4.2)) is satisfied.

Let $\bar{v} = 0$, $c_1 = -\log A$, $c_2 = -\alpha$ so that the equilibrium density (4.8) takes the form

$$p(v) = p_{\alpha,A,\theta}(v) = \frac{1}{A\,\exp(\alpha\,\|v\|^2)-\theta}\,, \tag{4.10}$$

where, according to (4.9),

$$A > \max(\theta, 0) \quad \text{and} \quad \alpha > 0\,. \tag{4.11}$$

Note that, in case $\theta > 0$ and $A \to \theta$, some delta-like distribution is obtained (Bose-Einstein condensation), while in case $\theta < 0$ and $A \to 0$, an approximate uniform distribution is obtained (Fermi level). For $A \to \infty$ distributions in both cases are close to a Maxwellian (with mean $\sim \frac{1}{A}$). Finally, in case $\theta = 0$, a pure Maxwellian is obtained. In the Fermi-Dirac case $\theta < 0$, the equilibrium density is bounded by $-\frac{1}{\theta}$. If the function $f(t,v)$ exceeds this bound, the gain term in equation (3.9) becomes zero so that the function decreases. One might expect that the correct equilibrium density is obtained even for initial densities f_0 that are not bounded by $-\frac{1}{\theta}$.

If the empirical density (2.14) exceeds the bound $-\frac{1}{\theta}$, then no more particles will come to the corresponding cell, but particles can leave that cell. So that, at steady state, the empirical density will satisfy the necessary condition (at least approximately as $N \to \infty$).

5. Numerical experiments

Since the equilibrium density is isotropic, it will be useful to consider the speed distribution, defined as

$$\tilde{p}(u) = \frac{4\pi u^2}{A\,\exp(\alpha\,u^2) - \theta}\,, \tag{5.1}$$

where $u = \|v\|$. Note that the speed distribution is mearly $p(v)$ given in (4.10) integrated over angle.

5.1. Fermi-Dirac case

Figure 1 shows the steady state speed distribution (5.1) measured in the simulation of a gas of Fermi-Dirac particles ($\theta = -1$). The parameters in this case are $A = 0.01$ and $\alpha = 1$ (cf. (4.11)), which corresponds to a temperature of $0.21\,T_F$ where T_F is the Fermi temperature [10]. The simulation used $N = 10^4$ particles and $M = 10^4$ velocity cells, which were cubic with a width of $\Delta v = 0.45$.[1] Note that for this choice of parameters we find good agreement with the expected equilibrium distribution.

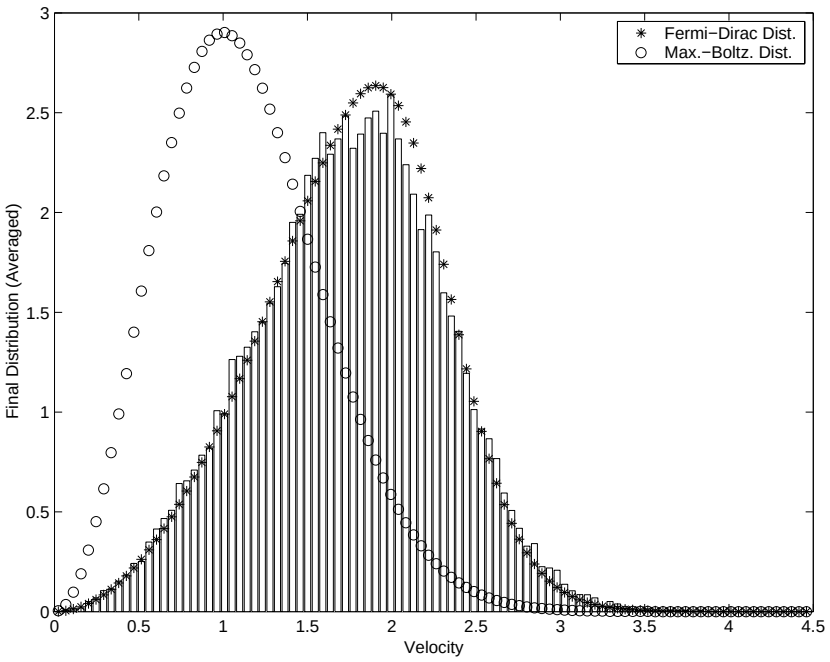

Figure 1: *Steady-state speed distribution in a Fermi-Dirac gas. Data from a simulation with $N = 10^4$ particles and $M = 10^4$ cells is shown as histogram bars; expected distribution shown by asterisks. The Maxwell-Boltzmann distribution for a gas with the same kinetic energy is shown, by open circles, for comparison.*

[1] Actually the value of M is rounded to the nearest cubic integer, e.g., for $M = 10^5$ the number of velocity cells is actually $97336 = 46^3$.

To quantify this agreement, the square integrated difference between the measured and expected speed distribution was evaluated as,

$$E(N,M) = \int_0^\infty [\tilde{p}(u) - \tilde{p}_s(u;N,M)]^2 \, du$$

where $\tilde{p}_s$ is the estimated steady state distribution from the simulation. For the results shown in Fig. 1 this error was 0.031. For comparison, a similar simulation for a Maxwell-Boltzmann gas (i.e., standard DSMC) had an integrated square difference of about 10^{-5}. As the value of E also varies with the parameters A and α, we use the normalized error defined as $\bar{E}(N,M) = E(N,M)/E(10^4,10^4)$.

Interestingly, increasing the number of velocity cells can *reduce* the accuracy of the distribution, as seen in **Figure 2**, which is similar to the previous figure but with the number of velocity cells increase to $M = 10^6$ (and the cell size reduced to $\Delta v = 0.09$). When the number of cells is significantly larger than the number of particles, Fermi exclusion is not accurately modelled.

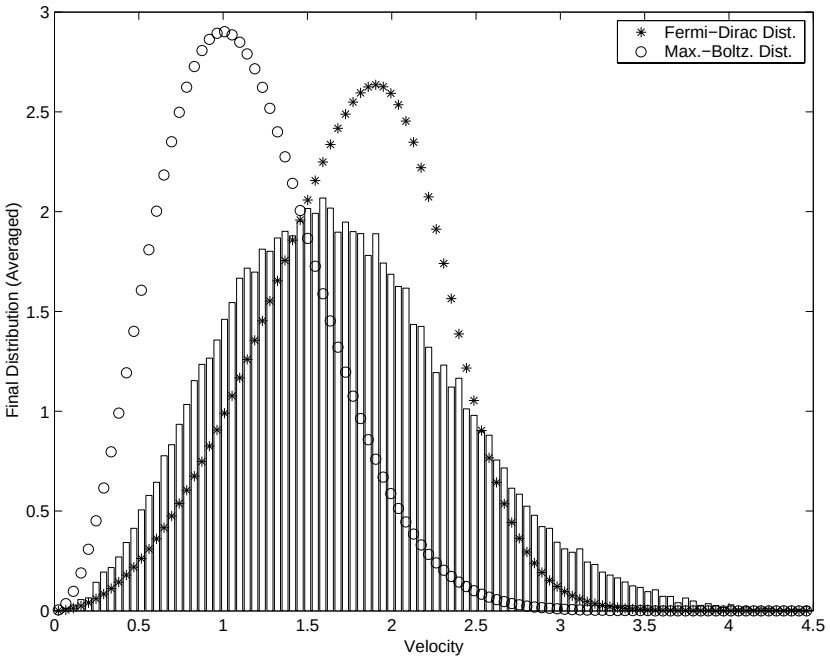

Figure 2: *Same as Figure 1 but for a simulation with $M = 10^6$ velocity cells.*

This effect is confirmed in **Figure 3**, which shows the normalized error as a function of the number of cells for various values of N. On the other hand, for a given number of cells the error plateaus when $N \geq M$, as shown in **Figure 4**. Roughly speaking, the error is minimum when $N \approx M$ and when we take the number of particles equal to the number of cells we find that the $\bar{E} \approx 1/M$, as shown in **Figure 5**. One also finds that even when $N = M \approx 300$ the distribution retains a strong quantum signature, when compared with the corresponding Maxwell-Boltzmann distribution (dashed line in **Figure 5**). Note that all of these results are for simulations using the parameters $A = 0.01$ and $\alpha = 1$; for different values of the parameters we expect quantitatively different errors (e.g., $\bar{E}$ decreases as A increases) but qualitatively similar dependence on N and M.

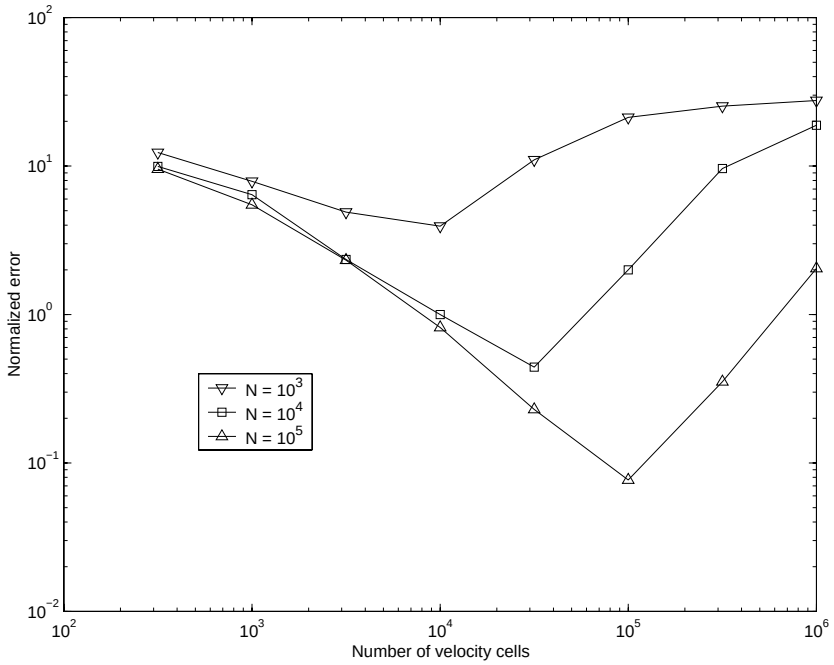

Figure 3: *Normalized error, $\bar{E}(N, M)$, in the steady-state Fermi-Dirac speed distribution as a function of the number of velocity cells.*

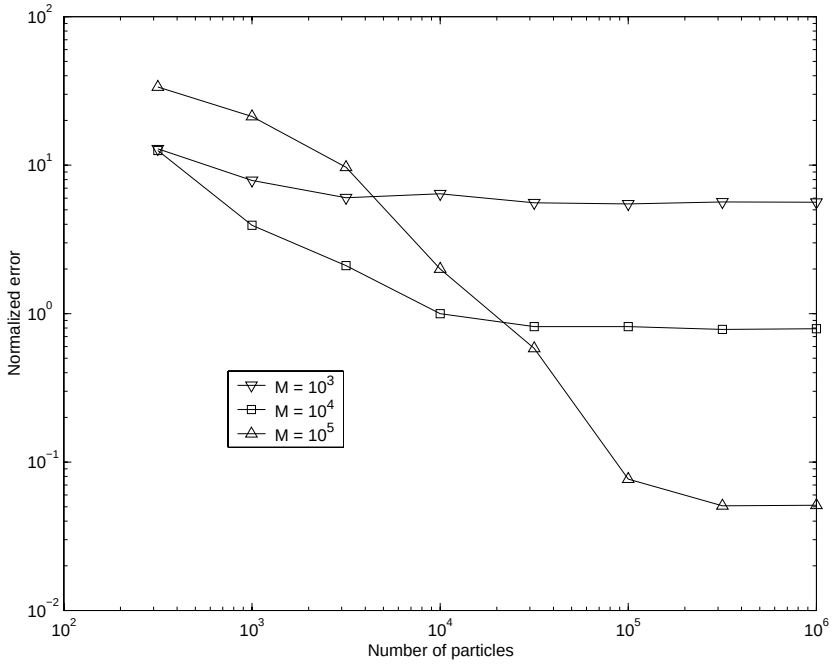

Figure 4: *Normalized error, $\bar{E}(N, M)$, in the steady-state Fermi-Dirac speed distribution as a function of the number of particles.*

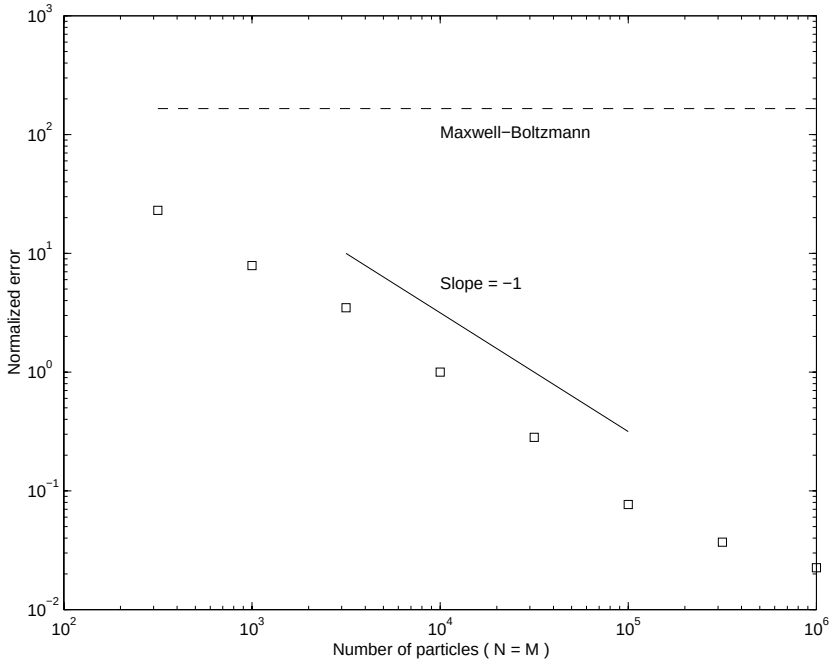

Figure 5: *Normalized error, $\bar{E}(N, M)$, in the steady-state Fermi-Dirac speed distribution as a function of $N = M$. For comparison, the error for a Maxwell-Boltzmann distribution (i.e., open circles in Fig. 1) is shown as a dashed line.*

5.2. Bose-Einstein case

Figure 6 shows the steady state speed distribution (5.1) measured in the simulation of a gas of Bose-Einstein particles ($\theta = 1$). The parameters in this case are $A = 1.01$ and $\alpha = 1$ (cf. (4.11)), which corresponds to a temperature of $1.08T_c$ where T_c is the critical temperature [10]. The simulation parameters are $N = 10^4$, $M = 10^4$ and $\Delta v = 0.38$. Although the agreement with the expected distribution is poor, **Figure 7** shows that the agreement is very good when N and M are increased to 10^6 (and Δv reduced to 0.08).

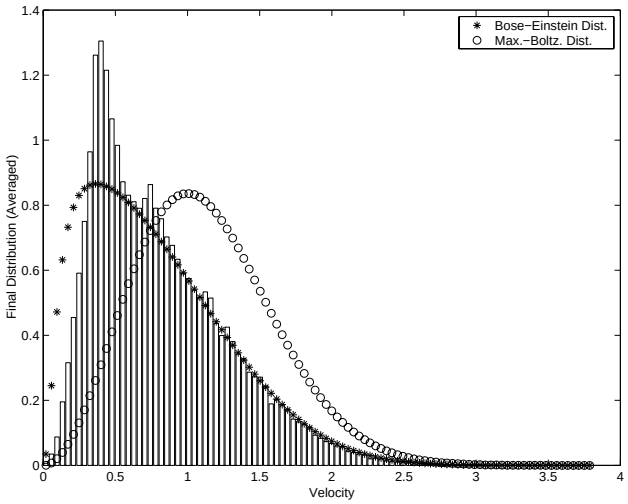

Figure 6: *Steady-state speed distribution in a Bose-Einstein simulation with* $N = 10^4$ *particles and* $M = 10^4$ *cells.*

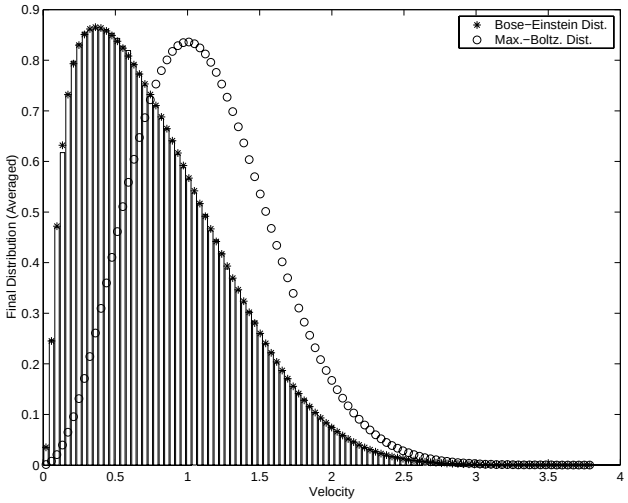

Figure 7: *Steady-state speed distribution in a Bose-Einstein simulation with* $N = 10^6$ *particles and* $M = 10^6$ *cells.*

Figure 8 shows that in these simulations of a Bose-Einstein gas, the normalized error drops with increasing number of particle cells until $M \approx 100N$. On the other hand, for a given number of cells $\bar{E}(N, M)$ is approximately constant in N, as shown in **Figure 9**, when $N > M/10$. Finally, graphing $\bar{E}(N, M)$ versus $N = M$ (**Figure 10**) shows that the error decreases roughly as $1/M$ except for small simulations ($M < 10^3$). For those simulations the error plateaus at approximately that of a DSMC simulation for a Maxwell-Boltzmann gas (i.e., $\theta = 0$), though the distribution is *not* Maxwellian. Again, all of the Bose-Einstein simulations used the parameters $A = 1.01$ and $\alpha = 1$; for different values of the parameters we expect quantitatively different errors (e.g., $\bar{E}$ decreases as A increases) but qualitatively similar dependence on N and M.

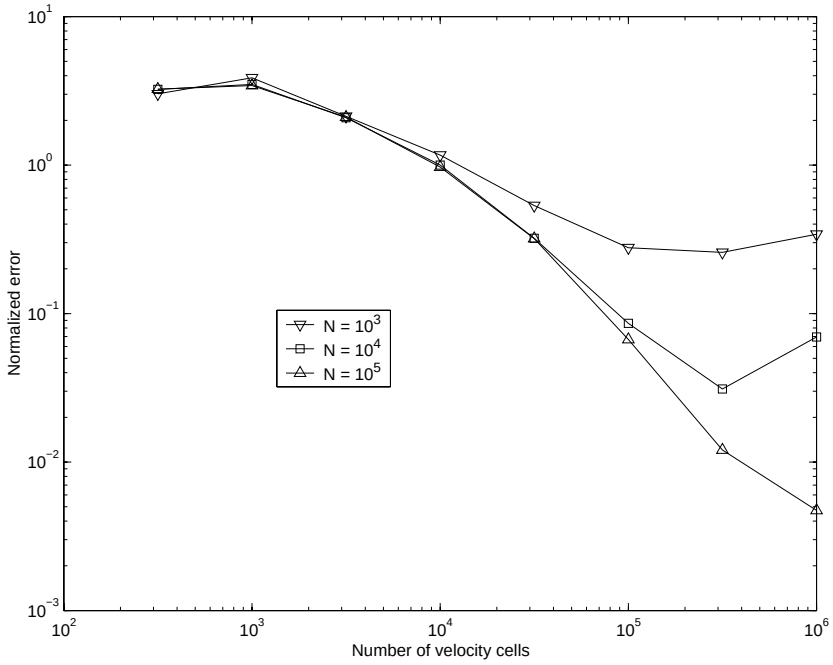

Figure 8: *Normalized error, $\bar{E}(N, M)$, in the steady-state Bose-Einstein speed distribution as a function of the number of velocity cells.*

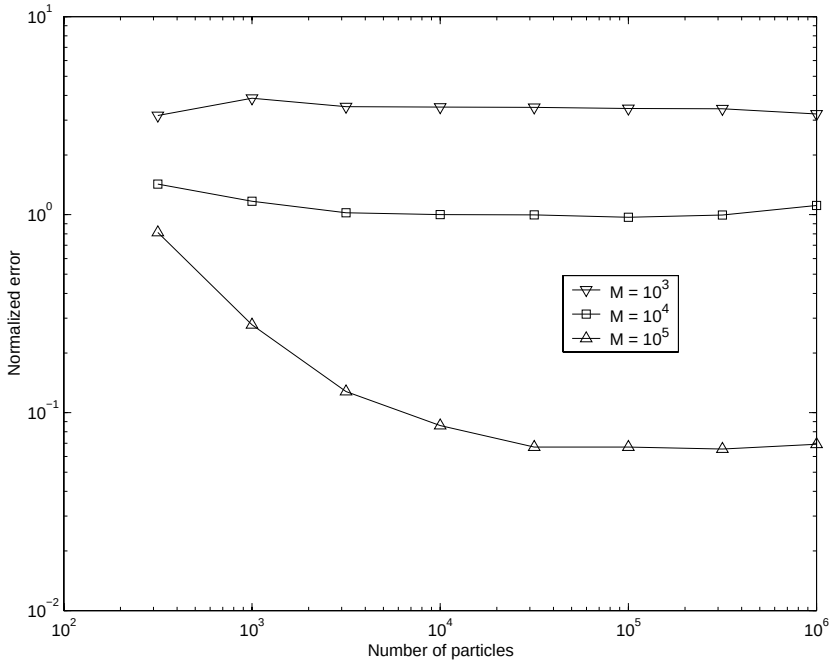

Figure 9: *Normalized error, $\bar{E}(N, M)$, in the steady-state Bose-Einstein speed distribution as a function of the number of particles.*

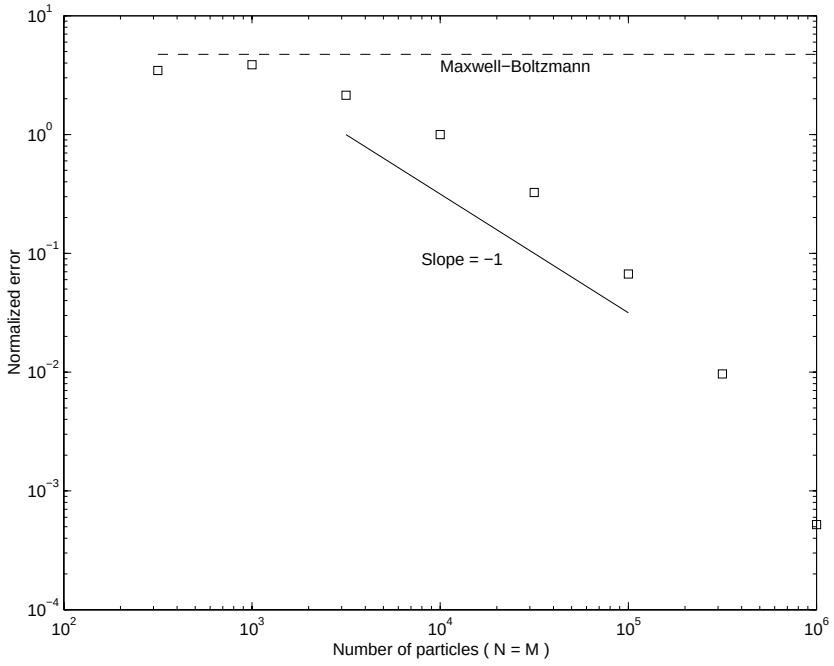

Figure 10: *Normalized error, $\bar{E}(N, M)$, in the steady-state Bose-Einstein speed distribution as a function of $N = M$. For comparison, the error for a Maxwell-Boltzmann distribution (i.e., open circles in Fig. 6) is shown as a dashed line.*

Acknowledgements

One of the authors (AG) wishes to thank the Weierstrass Institute for Applied Analysis and Stochastics, where this research was initiated, for its hospitality during his stay in Berlin. This work was supported, in part, by a grant from the European Commision DG 12 (PSS*1045) and was performed, in part, at Lawrence Livermore National Laboratory under the auspices of the Department of Energy under Contract No. W-7405-Eng-48.

References

[1] F. J. Alexander, A. L. Garcia, and B. J. Alder. A consistent Boltzmann algorithm. *Phys. Rev. Lett.*, 74(26):5212–5215, 1995.

[2] G. F. Bertsch and S. Das Gupta. A guide to microscopic models for intermediate energy heavy ion collisions. *Phys. Rep.*, 160(4):189–233, 1988.

[3] G. F. Bertsch, H. Kruse, and S. Das Gupta. Boltzmann equation for heavy ion collisions. *Phys. Rev. C*, 29(2):673–675, 1984. Erratum: Vol. 33(3), 1107 (1986).

[4] G. A. Bird. *Molecular Gas Dynamics and the Direct Simulation of Gas Flows*. Clarendon Press, Oxford, 1994.

[5] A. Bonasera, F. Gulminelli, and J. Molitoris. The Boltzmann equation at the borderline. A decade of Monte Carlo simulations of a quantum kinetic equation. *Phys. Rep.*, 243:1–124, 1994.

[6] E. Cerboneschi, C. Menchini, and E. Arimondo. Monte Carlo simulations of Bose-Einstein condensation of trapped atoms. *Phys. Rev. A*, 62:Article 013606, 2000.

[7] S. Chapman and T. G. Cowling. *The mathematical theory of non-uniform gases. An account of the kinetic theory of viscosity, thermal conduction and diffusion in gases.* Cambridge University Press, London, 1970.

[8] F. Dalfovo, S. Giorgini, L. Pitaevskii, and S. Stringari. Theory of Bose-Einstein condensation in trapped gases. *Rev. Modern Phys.*, 71:463–512, 1999.

[9] A. L. Garcia and W. Wagner. The limiting kinetic equation of the consistent Boltzmann algorithm for dense gases. *J. Statist. Phys.*, 101(5-6):1065–1086, 2000.

[10] K. Huang. *Statistical mechanics*. John Wiley & Sons Inc., New York, second edition, 1987.

[11] G. Kortemeyer, F. Daffin, and W. Bauer. Nuclear flow in consistent Boltzmann algorithm models. *Phys. Lett. B*, 374:25–30, 1996.

[12] A. Lang, H. Babovsky, W. Cassing, U. Mosel, H.-G. Reusch, and K. Weber. A new treatment of Boltzmann-like collision integrals in nuclear kinetic equations. *J. Comput. Phys.*, 106:391–396, 1993.

[13] R. L. Liboff. *Kinetic Theory: classical, quantum, and relativistic descriptions.* Wiley, New York, 1998. 2nd edition.

[14] X. Lu. A modified Boltzmann equation for Bose-Einstein particles: isotropic solutions and long-time behavior. *J. Statist. Phys.*, 98(5-6):1335–1394, 2000.

[15] K. Morawetz, V. Spicka, P. Lipavsky, G. Kortemeyer, C. Kuhrts, and R. Nebauer. Virial corrections to simulations of heavy ion reactions. *Phys. Rev. Lett.*, 82(19):3767–3770, 1999.

[16] E. A. Uehling and G. E. Uhlenbeck. Transport phenomena in Einstein-Bose and Fermi-Dirac gases. I. *Phys. Rev.*, 43:552–561, 1933.

[17] H. Wu, E. Arimondo, and C. Foot. Dynamics of evaporative cooling for Bose-Einstein condensation. *Phys. Rev. A*, 56:560–569, 1997.